논문 2006-43SC-1-5

클러터 환경에서 최적의 표적 추적을 위한 파형 파라미터와 검출문턱 값의 One-Step-Ahead 제어

(One-Step-Ahead Control of Waveform and Detection Threshold for Optimal Target Tracking in Clutter)

신 한 섭*, 홍 순 목**

(Han-Seop Shin and Sun-Mog Hong)

요 약

이 논문에서는 클러터 환경에서 최적의 거리와 거리방향 속도 추적을 위한 검출문턱값과 파형 파라미터의 one-step-ahead 제어를 제시하였다. 파형 파라미터의 최적 제어는 파형 파라미터에 대한 제약 조건이 있는 상황에서 추적 성능지수를 최소화하는 것이다. 성능지수는 항적분실확률과 추정오차 공분산행렬의 함수로 표현하였다. 항적분실확률과 오차 공분산행렬은 하이브리드 알고리듬을 이용하여 얻었다. 거짓 검출과 클러터 간섭의 영향은 이 성능 예측 알고리듬에서 함께 고려되었다. 여기서 제안한 one-step-ahead 제어의 추적 성능을 여러 가지 수치실험을 통해 확인하였고, 이 제어 방법은 유한 구간의 최적화 결과로부터 얻어진 경험적인 방법이다.

Abstract

In this paper, we consider one-step-ahead control of waveform parameters (pulse amplitudes and lengths, and FM sweep rate) as well as detection thresholds for optimal range and range-rate tracking in clutter. The optimal control of the combined parameter set minimizes a tracking performance index under a set of parameter constraints. The performance index includes the probability of track loss and a function of estimation error covariances. The track loss probability and the error covariance are predicted using a hybrid conditional average algorithm. The effect of the false alarms and clutter interference is taken into account in the prediction. Tracking performance of the one-step-ahead control is presented for several examples and compared with a control strategy heuristically derived from a finite horizon optimization.

Keywords: Optimal waveform selection, Tracking in clutter

I. Introduction

With the advent of flexible digital waveform generation techniques, many active radar and sonar systems are capable of adaptively generating waveforms for their transmitted pulses. The transmitted waveform has a significant effect on measurement accuracy and consequently on tracking performance. The waveform of a transmitted signal can be specified for a waveform class (e.g., Gaussian pulse) in terms of the waveform parameters which include pulse amplitude, pulse length, and FM sweep rate. Recently, attention has been focused on the question of optimal waveform parameter design to achieve optimum performance for target tracking. In [1, 2], waveform design was considered as an integral part of the overall tracking system design process.

* 정회원, 한국항공우주연구원 우주센터
(Space Center, Korea Aerospace Research Institute)
** 정회원, 경북대학교 전자전기컴퓨터학부
(School of Electrical Engineering & Computer Science, Kyungpook National University)
접수일자 : 2005년10월20일 수정완료일: 2006년1월9일

This integrated design achieved a significant improvement in the overall tracking performance. The optimum design of waveforms in transmitted pulses was extensively investigated in [3] and, more recently, in [4] on the basis of steady-state estimation performance.

In this paper, we consider one-step-ahead control of waveform parameters which minimizes a tracking performance index under a set of parameter constraints. In addition to the design of the waveform parameters, we also consider detection threshold selection as an integral part of the overall tracking system design process. The performance index includes the probability of track loss and a function of range and range-rate estimation error covariances. The track loss probability and the error covariances are predicted using a hybrid conditional average (HYCA) algorithm[5]. Specifically, we consider the case of a single Gaussian pulse and present a measurement model in explicit form which is developed based on the resolution cell in the delay-Doppler plane. We assume that the probabilistic data association (PDA) filter[6] is employed for tracking. The PDA filter is known to be robust against clutter, and performance evaluation algorithms exist. The effect of false alarms, clutter interference and the non-unity probability of target detection is taken into account in predicting PDA tracking performance using the HYCA algorithm. In order to determine the one-step-ahead control of the waveform parameters and detection threshold, first we compute the tracking performance indices on a set of feasible grid points in the control parameter space, and then choose the grid point (or the combined parameter set) with the smallest index as our one-step-ahead optimal control. A relatively coarse grid seems computationally efficient and enough to obtain a near-optimal control. Numerical experiments were performed to present tracking performance of the one-step-ahead control for several examples and to compare it with that of a control strategy heuristically derived from a finite horizon optimization.

Ⅱ. Sensor and Measurement Modeling

Assuming a return from a Swerling I target, we can obtain the relationship between the probability of detection (P_D), and the false alarm probability (P_F) such that

$$P_D(\tau, w) = P_F^{\frac{1}{1+SNR \cdot A(-\tau, w)}}. \quad (1)$$

Here, SNR is the signal-to-noise ratio which is the ratio of the expected value of the signal energy from target return to the noise spectral density. $A(-\tau, w)$ denotes the ambiguity function[3][7] for the actual return with time delay τ and Doppler shift w when a receiver filter is matched to a zero delay and a zero Doppler shift. To be more specific, we will focus on the case where the envelope function $s(t)$ is a linear frequency modulated (LFM) pulse with Gaussian amplitude modulation[7], that is,

$$s(t) = (\frac{1}{\pi\eta^2})^{1/4} exp(-(\frac{1}{2\eta^2} - jb)t^2) \quad (2)$$

where η is the pulse length parameter and b is the linear frequency sweep rate parameter. (The effective pulse length is determined by the point where the Gaussian pulse amplitude drops to 0.1 percent of the peak pulse amplitude, and is 7.4338η in the case of the Gaussian pulse[1].) Gaussian amplitude modulation suppresses ambiguity function sidelobes. The beneficial effects of amplitude modulation were discussed in [4]. In this case, the ambiguity function $A(-\tau, w)$ is given as[7]

$$A(-\tau, w) = \exp[-\frac{1}{2}(\frac{\tau^2}{\eta^2} + \eta^2(w - 2b\tau)^2)]. \quad (3)$$

Often the resolution cell in the delay-Doppler (τ, w) plane is defined in a tessellate shape, and it contains a region of P_D which is higher than a certain level[3]. The region can be expressed in terms of the ambiguity function and a corresponding parameter γ^2 as

$$R_C = \{(\tau, w) : A(-\tau, w) \geq \exp(-\frac{1}{2}\gamma^2)\}. \quad (4)$$

Clearly the region R_C is an ellipse in the case of an LFM Gaussian pulse. For the sake of simplicity, we approximate our resolution cell by the rectangle which encloses the ellipse R_C and is tangent to the sides. Using this approximation we develop a simple but reasonably accurate model of target detection and measurement. Let us denote the rectangular resolution cell by C. A typical shape of the resolution cell is shown in Fig. 1. The dots in the figure are the sampling grid, and for each sampling point a filter is matched to a replica of the envelop function $s(t)$ with a corresponding time delay and Doppler shift. The shaded area indicates the region where the detection probability for the sampling point at the origin is higher than for any other sampling point. The ellipse is the region R_C and the parallelogram indicates the resolution cell C. The resolution cell appears to be a parallelogram in this figure due to the different coordinate scales, but it is indeed a rectangle for identical scales. Notice that the resolution cell C well matches with the shaded region.

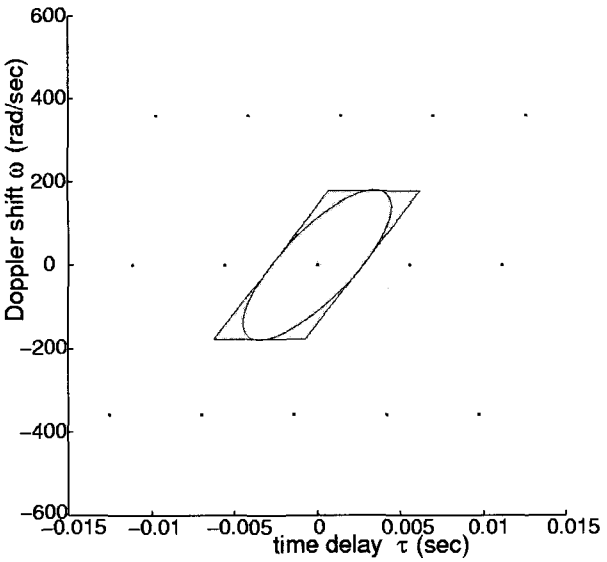

그림 1. 영역 R_C (타원), 분해셀 C (평형사변형)과 원점에서 샘플링 포인트의 검출확률이 다른 모든 샘플링 포인트보다 높은 확률을 가지는 영역 (그늘진 부분)

Fig. 1. Region R_C (ellipse), resolution cell C (parallelogram), and region (shaded area) that detection probability for the sampling point at the origin is higher than for any other sampling point (sampling points are denoted by dots in the figure).ease put the title of figure here.

The expected value of P_D in the cell C, denoted by $\bar{P}_D$, is

$$\bar{P}_D = \iint_C P_D(\tau, w) f(\tau, w) d\tau dw \Big/ \iint_C f(\tau, w) d\tau dw \quad (5)$$

where $f(\tau, w)$ is the probability density function of the target being at the coordinate (τ, w). We assume that the target location is uniformly distributed over the resolution cell C, i.e., $f(\tau, w)$ is uniform over C. Then

$$\bar{P}_D = \frac{1}{|C|} \iint_C P_D(\tau, w) d\tau dw \quad (6)$$

where C denotes the size of the cell C. The expected value $\bar{P}_D$ is an approximate probability of target detection of our tracking system. It is interesting to note that the size C of the rectangular cell is $4\gamma^2$ and it is invariant to the parameters η and b. If the signal-to-noise ratio SNR is sufficiently high, $SNR \cdot A(-\tau, w) \gg 1$ usually holds over C. Under this assumption that the signal-to-noise ratio is sufficiently high, we can use the approximation $1 + SNR \cdot A(-\tau, w) \approx (1 + SNR) \cdot A(-\tau, w)$. Substituting this approximation into (1) and substituting (1) into (6), we can obtain an approximate expression for $\bar{P}_D$ as

$$\bar{P}_D \approx P_{D0} a_1^2 \quad (7)$$

where $P_{D0} = P_F^{\frac{1}{1+SNR}}$ and $a_1 = \sum_{k=0}^{\infty} (\frac{1}{2}\gamma^2 \ln P_{D0})^k / ((2k+1) \cdot k!)$. The approximation of the series a_1 with up to third-order terms holds very accurately for a wide range of parameters. Notice that $\bar{P}_D$ depends on SNR, P_F and γ^2, but not on b.

We derived the measurement error covariance matrix in explicit form under the assumptions that $f(\tau, w)$ is uniform over C and that a target located in a given cell does not effect a detection in any

other cells. Under these assumptions, target detection takes place in proportion to $P_D(\tau, w)$ inside the resolution cell C, given that the target lies in the cell. Note that the coordinate of the sampling grid point of the cell C was assumed to be $(0,0)$ and it is the (location) measurement of target detection to be forwarded to the tracker. As a consequence, the measurement error of target detection is the random variables (τ, w) distributed in proportion to $P_D(\tau, w)$ over C. The covariance matrix of this error distribution is

$$R = \gamma^2 \frac{a_2}{a_1} \begin{pmatrix} \eta^2 & 2b\eta^2 \\ 2b\eta^2 & 1/\eta^2 + 4b^2\eta^2 \end{pmatrix} \tag{8}$$

where $a_1 = \sum_{k=0}^{\infty} (\frac{1}{2}\gamma^2 ln P_{D0})^k / ((2k+3) \cdot k!)$. The series a_2 is evaluated very accurately by the approximation with up to third-order terms, and the ratio a_2/a_1 can also be evaluated by the ratio of those approximations of a_1 and a_2. Although this measurement model is somewhat simplistic, it seems reasonably accurate for our characterization of tracking performance.

In [7], the sampling intervals of the output signal in time and in angular frequency have been suggested for a pulse with no frequency modulation as the inverse of the root-mean-square signal bandwidth and the inverse of the root-mean-square signal duration, respectively. For a Gaussian pulse, this pair of sampling intervals gives a resolution cell with size equal to 2. Our resolution cell C has size 2, if we choose

$$\gamma^2 = \frac{1}{2}. \tag{9}$$

Recall that the ellipse R_C inscribed in the cell C is specified by (4) with parameter γ^2. In the following section, we assume that the covariance matrix (8) is the measurement error covariance matrix of our measurement system, and assume that the probability of target detection is given by (7) with parameter (9).

Ⅲ. Tracker Characterization

Let us denote the state vector of a target by $\boldsymbol{x} = [r\dot{r}]^T$, where r and $\dot{r}$ denote target range and range-rate, respectively, and let us denote the measurement vector by $\boldsymbol{z} = [\tau w]^T$, where τ and w denote time delay and Doppler shift of target return, respectively. We assume the model described in [3] for target motion and measurements. The measurements are validated through a validation gate Z_G[3], and the volume of the validation gate is denoted by V_G. We also assume that the number of false measurements in the gate volume V_G approximately by a Poisson distribution with parameter λV_G, where $\lambda = P_F/|C| + \rho$ is the expected number of false measurements per unit volume. Here, ρ is the expected number of clutter measurements per unit volume in the $\tau - w$ plane.

Among various algorithms for tracking in clutter, we chose to use the PDA filter[6], which evaluates the posterior probabilities of associations. A HYCA algorithm has been developed in [5] in which the covariance matrix of the PDA filter is obtained by replacing the measurement dependent terms in the stochastic Riccati equation[6] with their conditional expectations evaluated only over possible locations of measurements in the validation region. This gives an approximate propagation of the covariance that retains its dependence on the number of the validated measurements.

For our PDA tracker characterization, we slightly modified the HYCA algorithm in order to obtain an approximate propagation of the covariance under the condition that the number of the validated measurements is maintained to be smaller than a certain integer M. The integer M is the tolerable limit on the number of validated measurements such that, if the number of validated measurements reaches or exceeds M at a certain time, the tracking filter is on the verge of losing track. We use this hybrid approximation in quantifying the estimation accuracy of PDA tracking. One cycle of this modified HYCA[8]

starts with given conditional expected value of the state covariance under the event that there were $m(k-1)$ validated measurements at $k-1$, denoted by $\bar{P}(k-1 \mid k-1, m(k-1))$, and a given conditional probability $P[m(k-1) \mid m(k-1) < M]$, denoted by $P'[m(k-1)]$. It updates the pair to give $\bar{P}(k \mid k), m(k))$ and $P'[m(k)]$. It also computes the average value of $\bar{P}(k \mid k, m(k))$ over $m(k)$, denoted by $\bar{P}(k \mid k)$, as

$$\bar{P}(k \mid k) = \sum_{m(k)=0}^{M-1} \bar{P}(k \mid k, m(k)) \cdot P'[m(k)] \quad (10)$$

and computes $P[m(k)]$ which is the conditional probability of the number of validated measurements at k being equal to $m(k)$ given that the number at any previous time is less than M. The cumulative probability of track loss through time k is given by

$$P_{TL}(k) = 1 - \prod_{i=1}^{k} \left(\sum_{m(i)=0}^{M-1} P[m(i)] \right). \quad (11)$$

In the following section, we use as a performance measure of PDA tracking, a weighted sum of the cumulative probability of track loss (11) and a function of the approximate covariance (10).

Ⅳ. Waveform Parameter and Threshold Optimization

Based on the measurement model and the tracker characterization developed in Sections Ⅱ and Ⅲ, we formulate a finite horizon optimization problem to minimize a performance index for PDA tracking. The sequence of the combined parameters $\theta(k) = (A(k), \eta(k), b(k), P_F(k))$ represents the parameters to be optimized. Notice that $A(k)$, $\eta(k)$ and $b(k)$ denote the peak amplitude, the length parameter and the linear frequency sweep rate of the transmitted pulse at scan k, respectively. $P_F(k)$ is the false alarm probability at the scan. First, let us define the index function for our optimization problem

$$J = c_1 P_{TL}(K) + c_2 \sum_{k=1}^{K} f(\bar{P}(k \mid k)), \quad (12)$$

where c_1 and c_2 are weighting factors and $f(\bar{P}(k \mid k))$ is a function of the approximate covariance $\bar{P}(k \mid k)$. The cumulative probability of track loss $P_{TL}(K)$ and the approximate covariance $\bar{P}(k \mid k)$ are evaluated by (11) and (10), respectively, to compute the index function J. Given the process noise spectral density σ_q^2, the index J is a function of the parameter sequence $\{\theta(k) \mid k = 1, 2, \cdots, K\}$.

We can now state that finite horizon optimization problem:

$$\min_{\{\theta(k) \mid k=1,2,\cdots,K\} \in \Theta} J \quad (13a)$$

subject to

$$\bar{P}(k \mid k, m(k)) = h_1(\{\bar{P}(k-1 \mid k-1, m(k-1)), P'[m(k-1)] \mid m(k-1) = 0, 1, \cdots, M-1\}, m(k), \theta(k)) \quad (13b)$$

$$P'[m(k)] = h_2(\{\bar{P}(k-1 \mid k-1, m(k-1)), P'[m(k-1)] \mid m(k-1) = 0, 1, \cdots, M-1\}, m(k), \theta(k)) \quad (13c)$$

for $m(k) = 0, \cdots, M-1$ and $k = 1, \cdots, K$. $\bar{P}(0 \mid 0, m(0))$ and $P'[m(0)]$ are given. The set Θ denotes a feasible set of the parameter sequence $\{\theta(k) \mid k = 1, 2, \cdots, K\}$. The constraint $\{\theta(k) \mid k = 1, 2, \cdots, K\} \in \Theta$ can include various limitations on the parameters, for instance, the maximum limits on the energy, amplitude, length, and FM sweep rate of transmitted pulses. The cumulative probability of track loss $P_{TL}(K)$, as a part of the index function (12), plays a role as a soft constraint on the probability of track loss. By setting K to one and solving the optimization problem at each scan, we obtain an one-step-ahead optimal control.

Ⅴ. Numerical Experiments

The optimization problem was solved numerically for several sonar-tracking scenarios. Limitations on the peak amplitude, length parameter, FM sweep rate, and

energy of transmitted pulses are imposed on the optimization as parameter constraints. First, let us assume that, for simplicity, $SNR = A^2\eta$. Under this condition we set limits on the energy (or SNR), amplitude, and length parameters of the transmitted (Gaussian) pulses as follows: $SNR \le SNR_{\max}$, $2.5 \times 10^{-3} \le \eta \le 2.5 \times 10^{-2}$ in sec, and $A \le 100$. The FM sweep rate is limited to an interval $b \le b_{\max}$ with $b_{\max} = 5\pi \times 10^3$ rad/sec^2. We consider the following four cases.

Case I: $\sigma_q^2 = 10^{-1}$, $\rho_0 = 10^{-2}$, and $SNR_{\max} = 63.1$ (18dB)
Case II: $\sigma_q^2 = 10^{-2}$, $\rho_0 = 10^{-2}$, and $SNR_{\max} = 63.1$ (18dB)
Case III: $\sigma_q^2 = 10^{-1}$, $\rho_0 = 0$, and $SNR_{\max} = 63.1$ (18dB)
Case IV: $\sigma_q^2 = 10^{-2}$, $\rho_0 = 10^{-2}$, and $SNR_{\max} = 15.8$ (12dB)

In the above, the power spectral density of the target process noise σ_q^2 and the spatial density of clutter ρ_0 have units of m^2/rad^3 and (rad)$^{-1}$, respectively. The density of clutter measurements ρ depends on many factors including the spatial clutter density ρ_0, clutter factors including the spatial clutter density ρ_0, clutter signal strength distribution, and detection threshold. Here, we performed numerical experiments for Rayleigh clutter. The signal-to-noise-ratio of clutter return is assumed to be $SNR/2$. In this case, $\rho(k) = \rho_0 P_F(k)^{\frac{1}{1+SNR(k)/2}}$.

In our experiments, we set the time between scans to 2 sec, the carrier (angular) frequency to $5\pi \times 10^4$ rad/sec, the speed of wave propagation to 1500 m/sec, $g = 4$ (that gives $P_G = 0.9997$ for 4-sigma gate on the two dimensional space), and $\gamma^2 = 1/2$ (that gives $C = 2$). M was set to 4. In the above, g is a parameter characterizing the size of the "g-sigma" ellipsoidal gate[6], and P_G denotes the probability that the target measurement falls inside the validation gate given that the target is detected. For $f(\bar{P}(k|k))$ in (12), we used $W\bar{P}(k|k)W^T$ where W is a weighting row vector $[1\ T]$. The function $W\bar{P}(k|k)W^T$ equals $\bar{P}_{11}(k|k) + 2T\bar{P}_{12}(k|k) + T^2\bar{P}_{22}(k|k)$, where $\bar{P}_{ij}(k|k)$ denotes the (i,j)-th element of $\bar{P}(k|k)$. This function represents a measure of the position estimation accuracy projected one-step-ahead in time. The weighting factors c_1 and c_2 were set to 1 and 10^{-3}, respectively.

In the finite horizon optimization, we set K to 40. Based on numerical solutions to this optimization, we proposed in [8]. a parameter switching strategy (denoted by SW) which is described in Table 1 for each case. The strategy SW switches between two sets of the combined parameters, depending on the value $\lambda(k)V_G(k)$ which is evaluated by using the parameters of the previous scan. We performed simulations of 50,000 Monte Carlo runs for the finite horizon optimization, the switching strategy SW, and the one-step-ahead control to evaluate their tracking performances over 40 scans. Constraint $SNR \le SNR_{\max}$ was always active in the finite horizon optimization. We select the pulse amplitude for SW so that SNR becomes $SNR_{\max}$. We obtained one-step-ahead optimal control by evaluating the index function J at 100 grid-points on the parameter space and by choosing

표 1. 각 Case에 대한 스위칭 방법 SW의 파형 파라미터
Table 1. Heuristic parameter switching strategy SW.

	$\lambda(k)V_G(k) \le 0.3$			$\lambda(k)V_G(k) \ge 0.3$		
	$\eta(k)$	$b(k)$	$P_F(k)$	$\eta(k)$	$b(k)$	$P_F(k)$
Case I	6.31×10^{-3}	$b_{\max}$	5×10^{-4}	6.31×10^{-3}	$-b_{\max}$	5×10^{-4}
Case II	1.25×10^{-2}	$b_{\max}$	4×10^{-5}	6.31×10^{-3}	$-b_{\max}$	6×10^{-4}
Case III	2.50×10^{-2}	$b_{\max}$	9×10^{-4}	6.31×10^{-3}	$b_{\max}$	4.5×10^{-4}
Case IV	1.25×10^{-2}	$b_{\max}$	2×10^{-3}	6.50×10^{-3}	$-b_{\max}$	4×10^{-3}

표 2. Case I에 대한 시뮬레이션 결과
Table 2. Simulation results for Case I.

	J	$P_{TL}(K)$	$\sum W\bar{P}(k\mid k)W^T$	steady-state rms range error (m)	steady-state rms range-rate error (m/sec)
Finite horizon optimization	0.504	0.210	2.94×10^2	1.087	0.359
SW	0.517	0.213	3.04×10^2	1.127	0.360
One-step-ahead control	0.537	0.178	3.59×10^2	1.265	0.373

표 3. Case II에 대한 시뮬레이션 결과
Table 3. Simulation results for Case II.

	J	$P_{TL}(K)$	$\sum W\bar{P}(k\mid k)W^T$	steady-state rms range error (m)	steady-state rms range-rate error (m/sec)
Finite horizon optimization	0.313	0.127	1.86×10^2	0.487	0.140
SW	0.315	0.137	1.78×10^2	0.471	0.136
One-step-ahead control	0.319	0.096	2.23×10^2	0.755	0.180

표 4. Case III에 대한 시뮬레이션 결과
Table 4. Simulation results for Case III.

	J	$P_{TL}(K)$	$\sum W\bar{P}(k\mid k)W^T$	steady-state rms range error (m)	steady-state rms range-rate error (m/sec)
Finite horizon optimization	8.95×10^{-2}	2.17×10^{-2}	6.78×10^1	0.544	0.212
SW	9.62×10^{-2}	2.22×10^{-2}	7.40×10^1	0.539	0.212
One-step-ahead control	8.94×10^{-2}	2.00×10^{-2}	6.94×10^1	0.523	0.209

표 5. Case IV에 대한 시뮬레이션 결과
Table 5. Simulation results for Case IV.

	J	$P_{TL}(K)$	$\sum W\bar{P}(k\mid k)W^T$	steady-state rms range error (m)	steady-state rms range-rate error (m/sec)
Finite horizon optimization	0.774	0.127	6.47×10^2	0.880	0.175
SW	0.761	0.164	5.97×10^2	0.848	0.175
One-step-ahead control	0.973	0.074	8.99×10^2	0.888	0.185

the parameter set that minimizes the index. Here, we also choose the pulse amplitude so that SNR becomes $SNR_{\max}$. Tables 2-5 list the simulation results of average values of J, $P_{TL}(k)$, and $\sum W\bar{P}(k\mid k)W^T$, and average rms errors of range and range-rate estimations. Although the index J for the finite horizon optimization and SW is not exactly the same quantity with the index that the one-step-ahead control minimizes, it provides an approximate but useful measure for performance comparison. Tables 2-4 shows that all control methods perform comparably to each other in Cases I-III. Table 5 indicates that one-step-ahead control is less effective in reducing the steady-state rms errors in Case IV. In our experiments, the advantages of one-step-ahead control over SW is not clear in terms of tracking performances. However, one-step-ahead control has advantages in that it can be more adaptive to tracking conditions and easier to implement in real-time. Notice that the switching strategy SW was heuristically obtained based on a parameter sequence a priori scheduled.

VI. Conclusion

In this paper, we consider one-step-ahead control of waveform parameters and detection thresholds for optimal range and range-rate tracking in clutter. The optimal control of the combined parameter set minimizes a tracking performance index under a set of parameter constraints. Tracking performance of the one-step-ahead control is presented for several examples and compared with a control strategy heuristically derived from a finite horizon optimization.

References

[1] D. J. Kershaw and R. J. Evans, "Optimal waveform selection for tracking systems," IEEE Transactions on Information Theory, vol. 40, no. 5, pp. 1536-1550, September 1994.

[2] D. J. Kershaw and R. J. Evans, "Waveform selective probabilistic data association," IEEE Transactions on Aerospace and Electronic Systems, vol. 33, no. 4, pp. 1180-1188, October 1997.

[3] C. Rago, P. Willett and Y. Bar-Shalom, "Detection-tracking performance with combined waveforms," IEEE Transactions on Aerospace and Electronic Systems, vol. 34, no. 2, pp. 612-624 April 1998.

[4] R. Niu, P. Willett and Y. Bar-Shalom, "Tracking considerations in selection of radar waveform for range and range-rate measurements," IEEE Transactions on Aerospace and Electronic Systems, vol. 38, no. 2, pp. 467-487, April 2002.

[5] X. R. Li and Y. Bar-Shalom, "Stability evaluation and track life of the PDAF tracking in clutter," IEEE Transactions on Automatic Control, vol. 36, no. 5, pp. 588-602, May 1991.

[6] Y. Bar-Shalom and T. E. Fortmann, Tracking and Data Association, Orlando, FL: Academic Press, 1988.

[7] H. L. Van Trees, Detection, Estimation, and Modulation Theory, Part III, New York: John Wiley, 1971.

[8] S.-M. Hong, R. J. Evans, and H.-S. Shin, "Optimization of waveform and detection threshold for range and range-rate tracking in clutter," IEEE Transactions on Aerospace and Electronic Systems, vol. AES-41, no. 1, pp.17-33, January 2005.

저 자 소 개

신 한 섭 (정회원)
1998년 경북대학교 전자공학과 학사
2000년 경북대학교 전자공학과 석사
2004년 경북대학교 전자공학과 박사
2004년 7월~현재 한국항공우주연구원 선임연구원
<주관심분야 : 레이다 추적 시스템, 최적화>

홍 순 목 (정회원)
현재 경북대학교 전자전기컴퓨터학부 교수